

Recent THM investigations on neutron induced reactions at astrophysical energies

Maria Letizia Sergi^{1,2}, Livio Lamia^{1,2}, Silvio Cherubini^{1,2}, Giuseppe D'Agata^{1,2}, Alessia Di Pietro², Juan Pablo Fernandez-Garcia², Pierpaolo Figuera², Giovanni Luca Guardo², Marisa Gulino^{2,3}, Seiya Hayakawa⁴, Iolanda Indelicato², Marco La Cognata², Marco La Commara^{5,6}, Dario Lattuada^{2,3}, Marcello Lattuada^{1,2}, Marco Mazzocco^{7,8}, Alessandro Alberto Oliva^{1,2}, Sara Palmerini^{9,10}, Rosario Gianluca Pizzone², Giuseppe Gabriele Rapisarda^{1,2}, Stefano Romano^{1,2}, Roberta Spartà², Claudio Spitaleri^{1,2}, Domenico Torresi², and Aurora Tumino^{2,3}*

¹Dipartimento di Fisica e Astronomia, via S. Sofia 64, I-95123 Catania, Italy

²INFN Laboratori Nazionali del Sud, Catania, Italy

³Università degli Studi di Enna “Kore”, Enna, Italy

⁴Center for Nuclear Study, University of Tokyo, Japan

⁵INFN-Sezione di Napoli, Napoli, Italy

⁶Dipartimento di Farmacia, Università di Napoli “Federico II”, Italy

⁷Dipartimento di Fisica e Astronomia, Univ. di Padova, Padova, Italy

⁸INFN-Sezione di Padova, Padova, Italy

⁹Istituto Nazionale di Fisica Nucleare, Sezione di Perugia, Via A. Pascoli s/n 06123, Perugia

¹⁰Dipartimento di Fisica e Geologia, Università degli Studi di Perugia, via A. Pascoli s/n 06123, Perugia

Abstract. Neutron induced reactions on stable and unstable nuclei play a significant role in the nucleosynthesis of the elements in the cosmos. In the last years, several efforts have been made to investigate the possibility of applying the Trojan Horse Method (THM) to neutron induced reactions mostly by using deuteron as “TH-nucleus”. Here, the main advantages of using THM will be given together with a more focused discussion on the recent $^7\text{Be}(\text{n},\text{o})^4\text{He}$ and the $^{14}\text{N}(\text{n},\text{p})^{14}\text{C}$ reactions.

1 Introduction

Neutron induced reaction play a key role in several astrophysical domains, ranging from primordial nucleosynthesis [1] to high mass nuclei stellar nucleosynthesis via the so-called *r*-process and *s*-process [2].

In the context of primordial nucleosynthesis, the cosmological lithium problem is one of the most challenging open questions in astrophysics and cosmology, introducing inconsistencies in the framework given by the standard Big Bang nucleosynthesis (BBN) for which primordial abundances are described by means of the only free baryon-to-photon ratio $\eta = n_b/n_\gamma$ parameter [3].

Possible solutions have been proposed, such as a different number of neutrino families or a revision of neutron lifetime. Among these, nuclear physics processes involving the unstable ^7Be ($t_{1/2} = 53.22 \pm 0.06$ days) are of particular interest. In more detail, at $\eta_{\text{CMB}} = (6.07 \pm 0.07) \times 10^{-10}$ [4] (value of η obtained through independent study on the cosmic microwave background (CMB) anisotropy) ^7Li is mainly produced from ^7Be that undergoes the electron capture process $e^- + ^7\text{Be} \rightarrow ^7\text{Li} + \nu_e$ at late times (i.e., long after the ^7Be synthesis). For this reason, ^7Be destruction channels are currently a matter of study because of their influence on

the ^7Li cosmological abundances. In particular, the (n,α) reaction channel has been the subject of recent works [5-8].

Regarding the *s*-process (where “*s*” stands for *slow*), when a neutron is captured, the resulting nucleus experiences β -decay to a more stable nucleus. The neutron capture time τ_n is higher than the half-life time τ_β of the unstable nucleus, thus ensuring the occurrence of β -decay before further neutron captures could occur. The $^{14}\text{N}(\text{n},\text{p})^{14}\text{C}$ reaction plays an important role in the *s*-process of nucleosynthesis: ^{14}N is very abundant since it is a dominant product of hydrogen-burning in the CNO cycle, the stage prior to the *s*-process. So, with its relatively high cross section, this reaction can act as a strong neutron poison in the reaction chain to heavier elements. Also, ^{14}N is of crucial importance in the nucleosynthetic origin of fluorine, whose only stable isotope is ^{19}F [9,10]. The He-burning shell in asymptotic giant branch stars is thought to be the most likely site for the synthesis of fluorine, mainly through the nuclear chain $^{14}\text{N}(\alpha,\gamma)^{18}\text{F}(\beta^+)^{18}\text{O}(\text{p},\alpha)^{15}\text{N}(\alpha,\gamma)^{19}\text{F}$.

In this sense, the $^{14}\text{N}(\text{n},\text{p})^{14}\text{C}$ reaction plays a key role since its double effect of *removing* neutrons and, at the same time, *producing* protons, captured by ^{18}O , that could trigger the $^{13}\text{C}(\text{p},\gamma)^{14}\text{N}$ which represents the competing channel of the neutron source $^{13}\text{C}(\alpha,\text{n})^{16}\text{O}$.

* Corresponding author: sergi@lns.infn.it

Here, we report first on the cross section measurement of the $^7\text{Be}(\text{n},\alpha)^4\text{He}$ performed via THM applied to the quasi-free $^2\text{H}+^7\text{Be}$ reaction and then on the preliminary results of the $^{14}\text{N}(\text{n},\text{p})^{14}\text{C}$ measurement by selecting the Quasi Free (QF) contribution to the $^2\text{H}(^{14}\text{N},\text{p})^{14}\text{C}$ reaction.

2 Basic features of THM

Nuclear reaction cross section measurements of interest for nuclear astrophysics are difficult to be performed in terrestrial laboratories mainly because of Coulomb barrier penetration and electron screening effects [11]. In order to overcome these difficulties, indirect methods, as THM and Asymptotic Normalization Coefficient (ANC) method [12], have been proved to be a valid complementary tool (see for example [13] and [14]) for experimental nuclear astrophysics since they allow the extraction of the astrophysically relevant cross section by selecting a precise reaction mechanism on a suitable reaction process thanks to devoted theoretical formalism.

The THM allows to obtain the cross section of a binary reaction $A(x,c)C$ of astrophysical interest for which direct measurements require the use of the extrapolation procedure to reach the relevant Gamow peak energy [15-19 and references therein].

In the last decades, the THM gave a relevant contribution to solve several problems, varying from pure nuclear physics to nuclear astrophysics.

The direct reaction mechanism approach is the basic theory of the THM, having its background in the research of the Quasi Free (QF) reaction mechanism [20-22].

By referring to the pole diagram of Fig. 1, nucleus a is chosen because of its large $a=x\oplus s$ configuration, its relatively low $x-s$ binding energy, and its known radial wavefunction for the $x-s$ configuration. It represents the so-called “Trojan-horse nucleus.” The three-body reaction is induced at energies well above the Coulomb barrier of the $A+a$ interacting particles in order to induce the sub-process $A-x$ in the nuclear field.

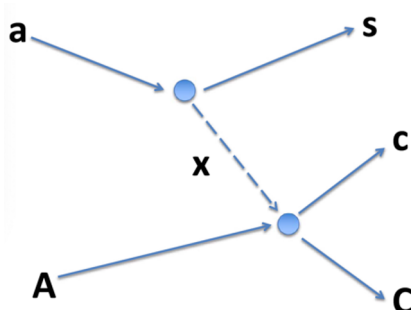


Fig. 1. Pole diagram for the quasi-free $a(A,cC)s$ reaction, s being the so-called spectator, while x represents the participant to the astrophysically relevant $A(x,c)C$ reaction.

Thus, the breakup of a is quasi-free because only cluster x takes part in the binary process, while the other counterpart s acts as spectator, i.e., it maintains in the

exit channel the same momentum distribution it had inside a before its break-up. In addition, a specific role is played by the $x-s$ binding energy, as pointed out in [15-19]: it compensates for the projectile energy down to low, i.e., astrophysically relevant, energies, thus making it of immediate help for nuclear astrophysics purposes. In particular, since the $A-x$ interaction occurs directly in the nuclear field, no Coulomb barrier penetration effects or screening phenomena [23] affect the THM data, in comparison with the direct impacts where these two effects cause the well known exponential decrease of the cross-section values and the enhancement of the cross-section values, respectively. In the most simple theoretical description of THM by means of the plane wave impulse approximation, the cross section of the quasi-free $a(A,c)C$ reaction can be related to the one of the binary $A(x,c)C$ processes via the formula [16,18]

$$\frac{d^3\sigma}{dE_c d\Omega_c d\Omega_C} \propto KF \cdot |\Phi(p_{xs})|^2 \cdot \frac{d\sigma}{d\Omega} \Big|_{\text{cm}}^{\text{HOES}},$$

where:

1. KF represents the kinematical factor, depending on the masses, momenta, and angles of the outgoing particles, that takes into account the final-state phase space factor.
2. $|\Phi(p_{xs})|^2$ is the square of the Fourier transform of the radial wavefunction describing the $x-s$ intercluster motion, usually in terms of Hänkel, Eckart, or Hulthén functions, depending on the $x-s$ system.
3. $d\sigma/d\Omega|_{\text{cm}}^{\text{HOES}}$ is the half-off-energy-shell (HOES) differential cross section for the two-body reaction at the center-of-mass energy $E_{\text{cm}} = E_{cC} - Q$, where Q represents the Q -value of the HOES $A(x,c)C$ reaction while E_{cC} represents the relative $c-C$ energy measured in laboratory. The deduced cross section is HOES because in the entrance channel, the transferred particle x having mass m_x is *virtual*, thus its energy and momentum are not related by the mass-shell equation $E_x = k_x^2/(2m_x)$.

Under QF conditions, the relative $A-x$ energy is then determined by relation $E_{Ax} = \frac{p_{Ax}^2}{2\mu_{Ax}} - \epsilon_{sx}$, with ϵ_{sx} being the binding energy of the TH -nucleus. In the exit channel, the relation is restored because the emitted $c-C$ particles are real (see [15-19] for details).

In recent past, an extension of the THM pointed out the ability of the method to also overcome the centrifugal barrier, measuring the bare nuclear cross section in neutron induced reactions [24-27].

In addition, a brand-new application of the method demonstrated the possibility to measure astrophysical relevant reaction cross section involving radioactive ion beams [28,29], with clear consequences in shedding light on research of neutron-induced reaction with unstable beams, usually tricky to perform with direct experiments [30]. In both the measurements described in the following sections, the deuteron was used as “trojan horse nucleus” because of its $p\oplus n$ cluster structure.

3 The $^7\text{Be}(\text{n},\alpha)^4\text{He}$ measurement

The $^2\text{H}(^7\text{Be},\alpha\alpha)\text{p}$ experiment was performed at the EXOTIC facility of Laboratori Nazionali di Legnaro (INFN-LNL) using a 20.4 MeV ^7Be beam impinging on a CD_2 target with a thickness of $400 \mu\text{g cm}^{-2}$. The detection setup was developed with the aim of detecting the two emerging alpha particles while the kinematical quantities of the undetected proton were reconstructed via momentum-energy conservation laws. In addition, since only quasi-free (QF) events were considered for the THM analysis, the setup covered the kinematical region corresponding to the QF-angular pairs, i.e., the angular pairs at which the spectator maintains the same momentum distribution it had inside the deuteron before its breakup [16,18].

The detailed description of the experimental set-up as well as the data analysis and the results have been already described step by step in [30], here only the resulting $^7\text{Be}(\text{n},\alpha)^4\text{He}$ reaction cross section is shown in Fig. 2 as blue filled square with corresponding statistical uncertainties.

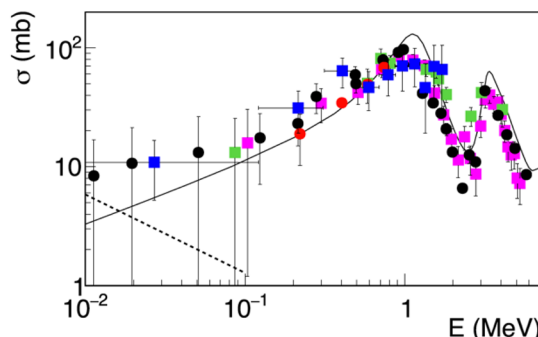


Fig. 2. THM $^7\text{Be}(\text{n},\alpha)^4\text{He}$ cross-section measurement (blue points with the statistical error) compared with the direct measurements [7] (red points) and [5] (black points). The magenta and green symbols refer to the reverse measurement obtained in [8]. The solid line is the ENDF/B-VII.1 evaluation [31] (<https://www.nndc.bnl.gov/sigma>), while the dotted line gives the trend of the direct radiative capture (DRC) cross section given in [6].

The THM data span a broad energy region, i.e., from ~ 30 keV up to ~ 2 MeV, providing the cross section in the region of interest for big bang nucleosynthesis. The THM investigation nicely overlaps with the direct data of [7] (red points), and at lower energies with the ones derived via CSH in [5]; black points). Additionally, the present results agree with the ones derived in [8] reported as green and purple filled squares. In the same figure, the dashed line refers to the evaluation of the total s-wave component for the present reaction as derived in [6] while the solid line represents the ENDF/B-VII.1 evaluation by [31].

The binary cross section extracted here by using the THM allowed us, for the first time, to span a wide range in energy in a single experiment overlapping both the high-energy region and the one of interest for BBN. In addition to the abovementioned agreement, also note that the present THM investigation significantly reduces the uncertainty in the BBN energy region, thus further

constraining the nuclear physics input for the cosmological lithium problem.

4 The $^{14}\text{N}(\text{n},\text{p})^{14}\text{C}$ measurement

The $^2\text{H}(^{14}\text{N},\text{p}^{14}\text{C})\text{p}$ experiment has been performed at Laboratori Nazionali del Sud of Catania (INFN-LNS). The SMP Tandem accelerator provided a 40 MeV ^{14}N beam with a spot size on target of about 1.5 mm and intensities up to 2-3 pnA. Deuterated polyethylene target (CD_2) of about $150 \mu\text{g/cm}^2$ was placed at 90° with respect to the beam axis. The experimental setup consisted of one $500 \mu\text{m}$ DSSSD (double sided silicon strips detectors) with an active area of $50 \times 50 \text{ mm}^2$ with 16 strips per side orthogonally oriented and one $1000 \mu\text{m}$ position sensitive detector (PSD) devoted to proton detection. They were placed at distance $d=28.4 \text{ cm}$ and $d=25.5 \text{ cm}$ from the target, respectively. The carbon particles were detected by means of a $\Delta\text{E-E}$ telescope (T) made of $20 \mu\text{m}$ strip detector as ΔE and $500 \mu\text{m}$ DSSSD as E-detector, placed at a distance $d=80 \text{ cm}$ from the target and placed on the opposite side with respect to the beam direction. The detectors covered the laboratory angles between 19.4° and 30.6° (DSSSD), between 35.0° and 45.0° (PSD) and between -3.2° and -6.8° ($\Delta\text{E-E}$ telescope).

As a first stage of the experiment, energy and angular calibrations of the adopted experimental equipment have been performed by means of 10 MeV, 20 MeV and 25 MeV ^{14}N beam impinging onto ^{197}Au , CD_2 , CH_2 thin targets as well as the use of a standard 8-peaks ^{228}Th alpha-source.

The reaction channel selection has been performed via the prior selection of the $Z=6$ locus in the $\Delta\text{E-E}$ telescope and the full kinematic reconstruction of the selected events with the hypothesis of a unitary mass for the third *undetected* particle. To validate the validity of the assumption, the experimental Q-value spectrum has been reconstructed and the result is shown as black points in Fig. 3. The agreement, within the experimental uncertainties, is a signature of a good detector calibration.

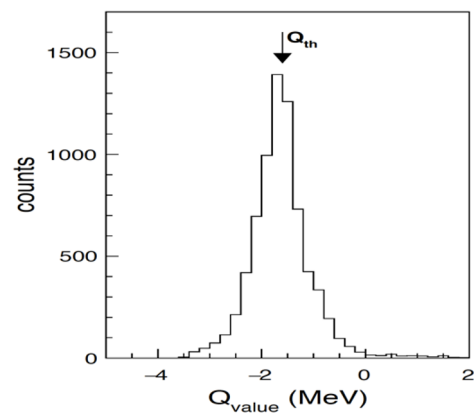


Fig. 3. Experimental Q-value spectrum. A peak centered at about -1.6 MeV , corresponding to the $^2\text{H}(^{14}\text{N},\text{p}^{14}\text{C})\text{p}$ channel. The black arrows correspond to the theoretical Q-value, $Q_{\text{th}} = -1.599 \text{ MeV}$.

Because the $^2\text{H}(^{14}\text{N}, \text{p}^{14}\text{C})\text{p}$ reaction has three particles in the exit channel, events from such reaction gather along a well-defined kinematic locus. By selecting the locus of interest, a kinematic identification of the reaction channel and, consequently, of the detected reaction products can be performed.

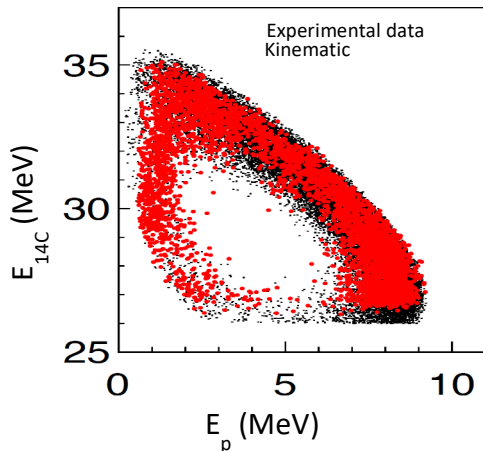


Fig. 4. Experimental kinematic locus (red circles) for the three-body $^2\text{H}(^{14}\text{N}, \text{p}^{14}\text{C})\text{p}$ reaction induced at $E_{\text{beam}} = 40$ MeV superimposed onto the simulated kinematical locus (black circles).

For this purpose, the energy correlation between ^{14}C and p only for the coincidences T-DSSSD is shown in Fig 4.

By comparison with the corresponding three-body kinematic calculation (black circles) it turns out that a single reaction channel contributes to the $E_{14\text{C}} - E_{\text{p}}$ correlation plot and the observed kinematic locus corresponds to the one for the $^2\text{H}(^{14}\text{N}, \text{p}^{14}\text{C})\text{p}$ three-body reaction.

As a further stage of the analysis, the identification of the QF-reaction mechanism is mandatory by studying, for instance, the shape of the spectator experimental momentum distribution (see [8] for details). Preliminary studies suggest the strong presence of such a reaction mechanism in the energy window of our interest. Further progress in data analysis is still required in order to obtain the cross section for the $^{14}\text{N}(\text{n}, \text{p})^{14}\text{C}$ reaction.

This research was funded by “Programma ricerca di ateneo UNICT 2020-22 linea2 (PIA.CE.RI 2020-22)” and by “Starting grant 2020” of the University of Catania.

5. S.Q. Hou, J.J. He, S. Kubono, Y.S. Chen, Phys. Rev. C, **91**, 055802, (2015)
6. M. Barbagallo, A. Musumarra, L. Cosentino, et al., PhRvL, **117**, 152701 (2016)
7. T. Kawabata, Y. Fujikawa, T. Furuno, et al., PhRvL, **118**, 052701 (2017)
8. L. Lamia, C. Spitaleri, C.A. Bertulani, et al., ApJ, **850**, 175, (2017)
9. M. Forestini, S. Goriely, A. Jorissen, M. Arnould, A&A **261**, 157 (1992)
10. G. D'Agata, et al., ApJ **860**, aac207, (2018)
11. C.E. Rolfs, W.S. Rodney, *Cauldrons in the Cosmos*, Eds: Chicago, Illinois, USA.: Univ of Chicago Pr, 1988
12. G.G. Kiss, et al., Phys. Lett. B **807**, 135606 (2020)
13. A. Caciolli et al., EPJA **52**, 136 (2016)
14. C. Spitaleri, et al., Phys. Rev. C **90**, 035801 (2014)
15. C. Spitaleri, et al., Phys. Atom. Nucl. **74**, 1725, (2011)
16. C. Spitaleri, et al., Eur. Phys. J. A **52**, 77, (2016)
17. C. Spitaleri, et al., Eur. Phys. J. A **55**, 161 (2019)
18. R.E. Tribble, C.A. Bertulani, M. La Cognata, A.M. Mukhamedzhanov, C. Spitaleri, RPPh, **77**, 106901, (2014)
19. M. La Cognata, et al., Journ Phys. C -Nuclear and Part. Phys. **35**, 014014 (2008)
20. G. Baur, PhLB **178**, 135, (1986)
21. M. Zadro, D. Miljanic, C. Spitaleri, et al. 1989, Phys. Rev. C, **40**, 181
22. G. Calvi, et al., Phys. Rev. C **41**, 1848, (1990)
23. H. Assenbaum, K.L. Langanke, C. Rolfs, ZPhyA, **327**, 461 (1987)
24. M. Gulino, et al., J. Phys. G Nucl. Phys. **37**, 125105 (2010)
25. M. Gulino, et al., Phys. Rev. C **87**, 012801, (2013)
26. G.L. Guardo, et al., Phys. Rev. C **95**, 025807, (2017)
27. G.L. Guardo, et al., Eur. Phys. J. A **55**, 211, (2019)
28. S. Cherubini, S. et al., Phys. Rev. C **92**, 015805, (2015)
29. R.G. Pizzone, et al., Eur. Phys. J. A **52**, 24, (2016);
30. L. Lamia, et al., ApJ **879**, 23, (2019)
31. M.B. Chadwick, et al., NDS, **112**, 2887 (2011)
32. S.Q. Hou, J.J. He, S. Kubono, Y.S. Chen, Phys. Rev. C, **91**, 055802, (2015)

References

1. R.G. Pizzone, et al., ApJ, **786**, 112, (2014)
2. C.A. Bertulani, *Nuclei in the Cosmos*, World Scientific, (2013), ISBN: 981441766
3. C.A. Bertulani, T. Kajino, PrPNP, **89**, 56, (2016)
4. P.A.R. Ade, N. Aghanim, M. Arnaud, et al. Planck Collaboration XIII, A&A, **594**, A13, (2016)